ISSN 0006-2979, Biochemistry (Moscow), 2021, Vol. 86, No. 8, pp. 1003-1011. © Pleiades Publishing, Ltd., 2021.
Russian Text © The Author(s), 2021, published in Biokhimiya, 2021, Vol. 86, No. 8, pp. 1207-1216.

# Structure and Function of Archaeal Translation Initiation Factor 2 Fragments Containing Cys2-Cys2 Motifs

**Oleg S. Nikonov[1,a]*, Natalia A. Nevskaya[1], Maria B. Garber[1], and Stanislav V. Nikonov[1]**

[1]*Institute of Protein Research, Russian Academy of Sciences, 142290 Pushchino, Moscow Region, Russia*
[a]*e-mail: alik@vega.protres.ru*

Received April 23, 2021
Revised May 21, 2021
Accepted May 25, 2021

**Abstract**—The heterotrimeric (αβγ) translation initiation factor 2 of archaea and eukaryotes (a/eIF2) supplies the P-site of the ribosome with the initiation tRNA. Its two subunits (β and γ) contain the Cys2-Cys2 motif, which is capable of forming a stable zinc finger structure in the presence of zinc ions. In this work, comparative analysis of the fragments containing Cys2-Cys2 motifs in the aIF2β and aIF2γ structures from different organisms was carried out and their environments in crystals was analyzed. Based on the obtained data, a conclusion was made that the conformation and role of these fragments in the β- and γ-subunits of the aIF2 are different.

**DOI**: 10.1134/S0006297921080101

*Keywords*: translation initiation factor 2, *Sulfolobus solfataricus*, crystal structure, zinc finger, Cys2-Cys2 motif

## INTRODUCTION

The classic zinc finger domain consists of two β-hairpins and one α-helix. The zinc atom coordinated with the Cys2-His2 motif [1] is located within the structure and stabilizes it. Non-classic types of zinc fingers can have other combinations of the coordinating atoms, in particular, Cys2-CysHis or Cys2-Cys2 [2]. The role of such structural domains in the cell is versatile. They are involved in recognizing DNA nucleotide sequence [3], can bind to RNA [4], as well as promote protein–protein interaction [5].

The translation initiation factor 2 of archaea and eukaryotes (a/eIF2) consists of three separate subunits (α, β, γ) and contains one Cys2-Cys2 motif in each β- and γ-subunits [6, 7]. The largest γ-subunit is functionally a GTPase. It is bound to the α- and β-subunits, whereas the latter two subunits do not contact with each other [8, 9]. During initiation process, the translation initiation factor in its active GTP-bound form participates in the translocation of the methionylated initiator tRNA ($Met\text{-}tRNA_i$) onto a small ribosomal particle [10]. After the codon-anticodon binding, GTP is hydrolyzed to GDP, and the factor in the inactive GDP-bound form leaves the ribosome leaving tRNA in its P-site.

Amino acid sequences of the β- and γ-subunits of a/eIF2 contain the Cys2-Cys2 motif, which in some cases coordinates a zinc ion. Thus, it was shown for the γ-subunit of the translation initiation factor 2 from *Pyrococcus abyssi* (PabIF2γ) that there is a structure in the region between the switches 1 and 2, which contains four closely located cysteines comprising a zinc finger. The presence of zinc atom in this structure was confirmed by atom-absorption spectroscopy [7]. Similar structures were found also in the γ-subunits of *Methanococcus jannaschii* (MjaIF2γ) [11] and *Pyrococcus furiosus* (PfuIF2γ) [12].

The zinc finger structure containing the Cys2-Cys2 motif and the coordinated zinc atom was also described in the structure of C-terminal domains of the β-subunits of the archaea *M. jannaschii* (MjaIF2β) [6] and *Methanobacterium thermoautotrophicum* (MbtIF2β) [13] determined by nuclear magnetic resonance (NMR), and of *P. furiosus* (PfuIF2β) [12] and *Sulfolobus solfataricus* (SsoIF2β) [8] determined by X-ray crystallography. According to classification presented in [14], zinc fingers (ZnF) of the a/eIF2 belong to the RanBP type because they consist of two β-hairpins containing four cysteines.

*Abbreviations*: a/eIF2, translation initiation factor 2 of archaea and eukaryotes; aIF2β, β-subunit of the archaeal translation initiation factor 2; aIF2γ, γ-subunit of the archaeal translation initiation factor 2; NMR, nuclear magnetic resonance.

* To whom correspondence should be addressed.

Similar structures have been described for a number of eukaryotic proteins, but their function is poorly understood, therefore, the role of zinc fingers in the a/eIF2 functioning has not been elucidated fully. At present, it is known that replacement of the second cysteine by serine in the γ-subunit [15] or disturbance of the integrity of the cysteine cluster in the β-subunit are critical for the cell growth and IF2 activity in the yeast systems [16]. Some mutations in the β-subunit increase the rate of GTP hydrolysis in yeast and make it independent on the eIF5 [17]. Deletion of the zinc-binding motif in the β-subunit leads to defects in the translation initiation [18].

Among the all known aIF2 structures, the SsoIF2γ structure is the most studied. The structure of this subunit has been investigated in all functional states: the GTP-bound, the GDP-bound, and the nucleotide-free state [19]. Moreover, the structures of heterodimers αγ [20], βγ [12], and of the incomplete (containing fragments of the α- and β-subunit and the full γ-subunit) and of the complete αβγ-heterotrimer [8, 9] are also known. The produced crystals belong to different groups of spatial symmetry, which makes it possible to study in detail protein–protein interactions specific for the Cys2-Cys2 motif of this subunit.

In the present work, it was attempted to summarize the available information about the structural fragments of the β- and γ-subunits of a/eIF2 containing the Cys2-Cys2 motifs and possessing the conformation corresponding to the RanBP type zinc fingers. The structure of the motif from the γ-subunit of *S. solfataricus* was found to be fundamentally different from the structures in the other aIF2γ. Based on the study of the known structures and their arrangements in the crystal, the following conclusions are made:

1) The zinc finger of the β-subunit is necessary for additional protection of GTP in the nucleotide-binding pocket and for decrease in the internal GTPase activity of the factor. The sulfur atoms of the β-subunit four cysteines in all known structures are located in the apices of the regular tetrahedral pyramid with a coordinating zinc ion in its center, whereas the C-terminal domain of the subunit that contains them exhibits high lability. The ordered structure of the zinc finger of this subunit cannot exist without the coordinating zinc ion;

2) The Cys2-Cys2 motif in the γ-subunit is a part of the subdomain, which forms the β-subunit binding site. In the known structures of the archaeal aIF2γ, the subdomain either has a zinc finger conformation, or, as in the γ-subunit of SsoIF2, forms two stabilizing S-S bonds between the neighbor hairpins and is unable to bind zinc ion. In the latter case, the subdomain conformation is determined by amino acid sequences after the second and fourth cysteines;

3) Presence of the Cys2-Cys2 motif in the amino acid sequence is not sufficient condition for formation of the zinc finger structure.

## MATERIALS AND METHODS

In the work the structures of free β- and γ-subunits of the translation initiation factor 2 of archaea were used as well as of their complexes determined by methods of X-ray crystallography and NMR (table). All structures were taken from the PDB database. The border of the zinc finger domain in the β-subunits was determined at two amino acid residues (aa) before the first cysteine, as it was done in the previous works [6]. In the γ-subunits, the subdomains containing the Cys2-Cys2 motifs, also begin two aa before the first cysteine.

The sequences were superimposed manually using the data of the structure. Fragments of the structures were superimposed using the O program [21].

## RESULTS

It was shown earlier [8, 11, 12] that the structures of the β- and γ-subunits of aIF2 from different organisms have a high degree of similarity, especially in some elements of the secondary structure. Therefore, for the convenience, the structure of the βγ-complex from *P. furiosus* (PDB-code: 2d74) is presented in Fig. 1 with the indicated structural elements discussed in the text of the article. Fragments of the β- and γ-subunits containing the Cys2-Cys2 motifs are indicated with half-transparent spheres and the Cα-atoms are indicated with white spheres. According to the existing practice, the short β-hairpins of the Cys2-Cys2 fragments are not shown in Fig. 1. These hairpins marked with prefix f (e.g., fβ1) are shown in comparison of the sequences of the fragments from different organisms.

**Zinc fingers in the β-subunits of aIF2.** As mentioned earlier, the structures of C-terminal domains of the aIF2β containing the Cys2-Cys2 motifs are known for four organisms: *M. jannaschii* [6], *M. thermoautotrophicum* [13], *P. furiosus* [12], and *S. solfataricus* [8]. Sequences of these domains contain 35 aa and can be described by the same common formula: 2x, C, 2x, C, 17x, C, 2x, C, 8x, where x is any aa. The sequence of *S. solfataricus* has the highest number of substitutions (33.3% identity with the other sequences), whereas identity of the sequences from *M. jannaschii*, *P. furiosus*, and *M. thermoautotrophicum* is 54.5%, and for the sequences of the C-terminal domains MjaIF2β and PfuIF2β the identity reaches 70%.

All C-terminal domains of the β-subunits of the above-mentioned structures have the zinc finger conformation with zinc atom in the middle of the tetrahedral regular pyramid and sulfur atoms located in its apices. The edge of the pyramid in the structures determined by the NMR method is 3.81 ± 0.02 Å, whereas the edges in the structures determined by X-ray crystallography show a somewhat lower average length and a significantly

Structures of aIF2 and its subunits used in the work

| Object | Ligand | PDB-code | Method | Symmetry group | Resolution, Å | Reference |
|---|---|---|---|---|---|---|
| SsoIF2γ | GDP | 2pmd | X-ray | $P3_1$ | 2.65 | [22] |
| SsoIF2(αγ) | GDPNP | 2aho | X-ray | $P2_12_12_1$ | 3.00 | [20] |
| $SsoIF2(\alpha\beta\gamma)_{incomp}$ | GDP | 2qn6 | X-ray | $C_12_1$ | 2.15 | [8] |
| SsoIF2γ(Δ37-47) | GDP | 3pen | X-ray | I23 | 2.30 | u/p |
| SsoIF2γ | GDPCP | 4rjl | X-ray | I23 | 1.64 | [23] |
| SsoIF2γ | GDPNP | 4rd4 | X-ray | $P2_12_12_1$ | 1.30 | [24] |
| SsoIF2γ | GDP | 4rd6 | X-ray | $P2_12_12$ | 1.94 | [24] |
| SsoIF2γ+formate | GDP | 4m4s | X-ray | H32 | 2.25 | [19] |
| SsoIF2γ | GDP | 4m0l | X-ray | $P2_1$ | 2.60 | [19] |
| SsoIF2γ | – | 4m2l | X-ray | $P3_12_1$ | 2.15 | [19] |
| SsoIF2γ | GDPCP | 4m53 | X-ray | I23 | 2.00 | [19] |
| $SsoIF2\gamma(-Mg^{2+})$ | GDPCP | 6h6k | X-ray | P1 | 2.00 | [25] |
| PfuIF2(βγ) | GDP | 2d74 | X-ray | $P2_12_12_1$ | 2.80 | [12] |
| PabIF2γ | GDP | 1kk3 | X-ray | $P2_1$ | 1.90 | [7] |
| MjaIF2γ | – | 1s0u | X-ray | $P2_1$ | 2.40 | [11] |
| MjaIF2β | – | 1k81 | NMR | i/a | i/a | [6] |
| MbtIF2β | – | 1nee | NMR | i/a | i/a | [13] |
| SsoIF2αβγ | – | 3cw2 | X-ray | $P2_1$ | 2.80 | [9] |
| SsoIF2αβγ+tRNA | GDPNP | 3v11 | X-ray | P3221 | 5.0 | [26] |

Notes. Designations: Sso, *S. solfataricus*; Pfu, *P. furiosus*; Pab, *P. abyssi*; Mja, *M. jannaschii*; Mbt, *M. thermoautotrophicum*; GDP, guanosine diphosphate; GDPCP, 5′-guanosylmethylene triphosphate; GDPNP, 5′-guanilylimido-diphosphate; incomp, incomplete complex; X-ray, X-ray crystallography; NMR, nuclear magnetic resonance; formate, formiate; u/p, unpublished; i/a, inapplicable.

greater variations (3.43 ± 0.25 Å), possibly, because of the rather low resolution. The zinc atom position in these structures is also different from its ideal coordination observed in the NMR-structures. However, it should be noted that slight rotations of the sulfur atoms of the cysteines around the Cα-Cβ bond make it possible to arrange them in the apices of the regular tetrahedral pyramid without leaving the electron density limits.

It was shown earlier that zinc is required for stabilization of the C-terminal domain of aIF2β [27]. The structure of the complete factor [9] confirms that the absence of zinc atom in the crystallization solution leads to disordering of this domain. The most clear representation of the secondary structure of the zinc finger can be obtained by analyzing the NMR-derived structure of the MjaIF2β fragment (PDB-code: 1k81) [6], because this fragment is free of distortions caused by the packing of molecules in the crystal. The base of the zinc finger structure is an antiparallel β-sheet consisting of three β-strands (Fig. 2). The β-hairpin formed by two last β-strands contains two cysteines. Two other cysteines in the composition of the zinc finger are at the ends of the distorted helix containing a single turn with axis parallel to the β-sheet surface. Unlike in the NMR-derived structures, the crystal structures contain two β-hairpins (h1-h2, h3-h4), with two cysteines in each. The hairpins are arranged in two approximately parallel planes; the zinc ion is located between them. The zinc finger surface is mainly hydrophobic, however, a significant number of oxygen atoms of the major chain are accessible for the solvent molecules in the cysteine cluster region.

Despite the high degree of identity (67%) of the amino acid sequences and the identical mutual arrangement of sulfur atoms, superposition of the NMR-derived structures (MjaIF2β and MbtIF2β) is associated with the difficulties, because interaction of the N-terminal domain of the β-subunit with its central domain in one of them [27] leads to dramatic distortions in the structures of both the β-sheet and the N-terminal part of the zinc finger. The crystal structures of the zinc fingers of the

β-subunits from SsoIF2 and PfuIF2 also demonstrate a high lability, however, in these structures the β-hairpins (h1-h2 and h3-h4) retain their conformation (Fig. 3). Mutual arrangement of the Cα-atoms and sulfur atoms of all four cysteines is also retained within the margin of experimental error. However, conformation of the central part of the zinc finger changes significantly depending on the position of the C-terminal part relative to the γ-subunit. The γ-subunit region containing the nucleotide-binding pocket is covered by the zinc finger of the β-subunit (SsoIF2), or by its central domain (PfuIF2); in both cases, the bound nucleotide is protected.

The zinc finger of the β-subunit in crystals of the βγ-heterodimer PfuIF2 [12] and of the incomplete heterotrimeric complex SsoIF2 [8] has different environment and interacts with different regions of the γ-subunit symmetric molecule. In crystals of the incomplete SsoIF2βγ3Dα heterotrimer [8], the zinc finger of the β-subunit is shifted to the domain III of the γ-subunit and essentially covers the nucleotide-binding pocket. The difference in the crystal packing of these two structures is, apparently, the main cause of the changes in the conformation of their zinc fingers.

It should be noted that the structures of the β-subunit zinc finger have significantly different conformations in the crystal and in the solution. It has been mentioned already that it is impossible to compare the two structures obtained by the NMR method. An attempt to superimpose β-hairpins of the crystal structures onto the regions of the structures with the corresponding amino acid sequence in solution, at best, makes it possible to obtain standard deviation of ≈3 Å with pronounced displace-

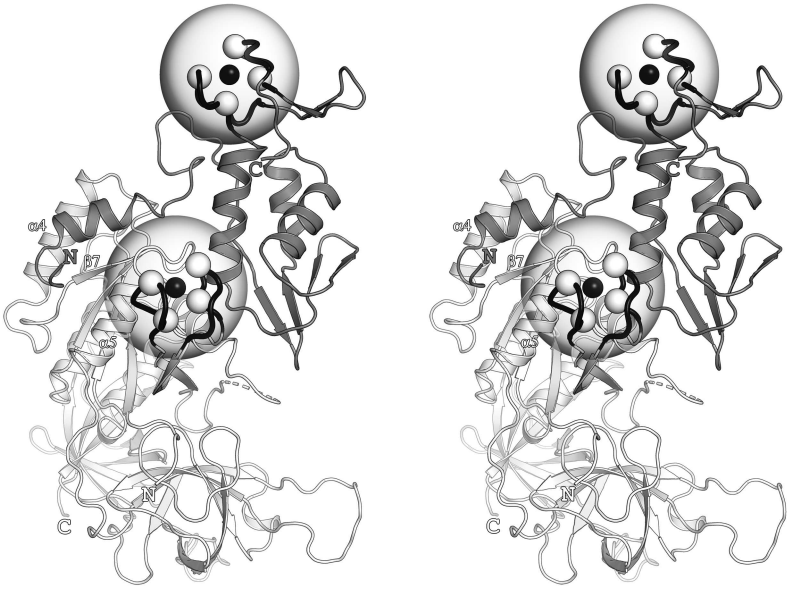


**Fig. 1.** Structure of the aIF2βγ complex from *P. furiosus* (PDB-code: 2d74); stereopairs. Elements of the secondary structure and functionally important regions are shown, which are discussed in the text. Structures of the β- and γ-subunits are shown in white and gray colors, respectively. Zinc-binding motifs are indicated with half-transparent spheres. The Cα-atoms of cysteines are shown as white spheres, zinc ions are shown as black spheres, the polypeptide chain, which forms the zinc-binding motifs, is shown with black color.

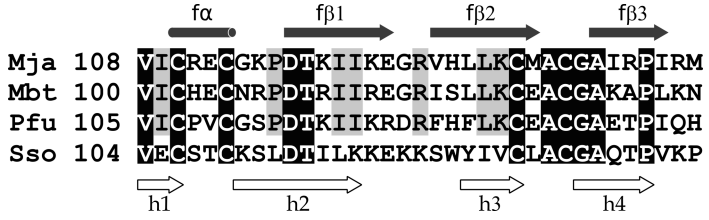


**Fig. 2.** Comparison of amino acid sequences of zinc fingers of the β-subunits from *M. jannaschii* (PDB-code: 1k81), *M. thermoautotrophicum* (PDB-code: 1nee), *P. furiosus* (PDB-code: 2d74), and *S. solfataricus* (PDB-code: 2qn6). Amino acid residues common for all the four sequences are shown in white color on the black background, and those common for three sequences except the SsoIF2β sequence are shown on the gray background. The α-helix and three long β-strands correspond to the zinc finger of MjaIF2β, the β-hairpins (h1-h2 and h3-h4) correspond to the zinc fingers of *P. furiosus* and *S. solfataricus*.

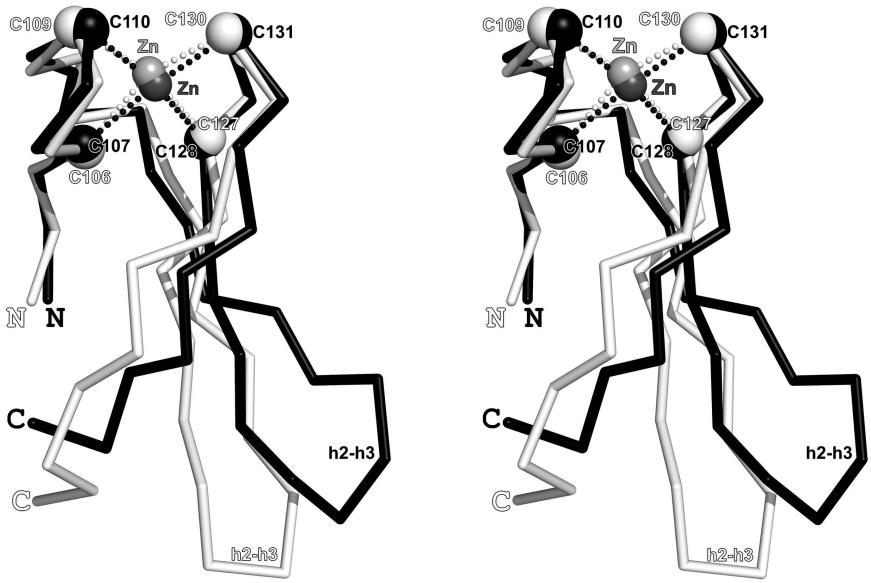


**Fig. 3.** Superposition of the crystal structures of zinc fingers of the β-subunits from the SsoIF2 (shown in white color, PDB-code: 2qmu) and PfuIF2 (shown in black color, PDB-code: 2d74); stereopairs. Superposition is performed for 17 Cα-atoms [103-113 (104-114) and 127-132 (128-133)] in the SsoIF2 and PfuIF2, respectively; the Cα-atoms are shown as white and black spheres, respectively, with σ = 0.534 Å. All four cysteines occupy approximately the same positions in the two structures (maximum deviation of the Cα-atoms in the Cys106-Cys107 pair is 0.64 Å), whereas positions of the β-hairpin h2-h3 and the C-terminal part of the finger are very different and are fully determined by the crystal packing. Zinc ions are shown as light-gray (2qmu) and dark-gray (2d74) spheres.

ments of the Cα-atoms of all four cysteines. Thus, even in the presence of the coordinating zinc ion, the zinc finger of the β-subunit is a highly labile structure and is capable of acquiring different conformations.

**Zinc fingers in the aIF2γ structures.** Zinc atom in the structures of γ-subunits from *P. abyssi* [7], *P. furiosus* [12], and *M. jannaschii* [11] coordinates four sulfur atoms, as it is observed also in the β-subunits. A fragment of the structure containing the Cys2-Cys2 motif is a subdomain linked to the molecule body by two β-strands and is described by the common formula: 2x, C, 2x, C, 8x, C, 2x, C, 6x. The zinc fingers of PabIF2γ and PfuIF2γ are identical, except one residue. Identity of sequences of the zinc fingers of PabIF2γ and MjaIF2γ is 67%.

Similarly to the zinc fingers of the β-subunit crystal structures, the zinc fingers of the three γ-subunits under consideration are also formed by two β-hairpins (Fig. 4). The hairpins are linked by the second order symmetry axis, which passes through the zinc atom and is approximately parallel to the axis of the finger. There are four oxygen atoms of the major chain on the plane surface of every hairpin, which are exposed to the solvent. The cysteine containing regions of the zinc fingers in the β- and γ-subunits crystal structures have similar conformations. In particular, they can be superimposed on each other in the PfuIF2βγ structure with the mean standard deviation 1.05 Å for 18 Cα-atoms, whereas for nine N-terminal Cα-atoms this value is decreased to 0.47 Å. The region between the N-terminal and C-terminal pairs of cysteines in the γ-subunits is two times shorter than in the β-subunits, that, apparently, essentially affects stability of the zinc finger structure.

The β-hairpin containing the C-terminal pair of cysteines has a close contact with the central domain of the β-subunit in the PfuIF2γ crystal, whereas the apex of the hairpin containing the N-terminal pair of cysteines contacts with the α1-helix of the β-subunit. Both the apex of the C-terminal hairpin and the apex of the N-terminal hairpin have contacts with the surrounding

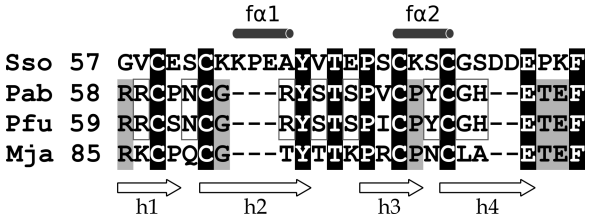


**Fig. 4.** Comparison of the Cys2-Cys2 amino acid sequences of the subdomains of the archaeal IF2γ *S. solfataricus* (PDB-code: 4rd4), *P. abyssi* (PDB-code: 1kk3), *P. furiosus* (PDB-code: 2d74), and *M. jannaschii* (PDB-code: 1s0u). The single-turn helices in the SsoIF2γ structure are shown as fα1 and fα2, β-hairpins – as h1-h2 and h3-h4. The residues, which coincide in all four cases are shown in white on the black background, those that coincide in three cases – are shown on the gray background, and those that coincide only in two cases – are marked with the gray rectangles.

molecules in the PabIF2γ and MjaIF2γ crystals, respectively. Never-theless, all the 24 Cα-atoms, which form the zinc finger of the indicated structures, can be superimposed on each other with the standard deviation not higher than 0.57 Å.

There are several PabIF2γ structures in the PDB database, which have been determined with the resolution better than 1.9 Å. These structures make it possible to assess the mean distance between the sulfur atoms coordinated by zinc as 3.69 ± 0.25 Å that is close to the assessment of this value in the aIF2β structures based on the data produced by NMR. It should be noted that the change in conformation of the side chains of cysteines in these structures within the electron density limits makes it possible to easily arrange the sulfur atoms in the apices of the regular tetrahedral pyramid.

**The Cys2-Cys2 motif in the SsoIF2γ structure.** The cysteine cluster of SsoIF2γ involves amino acid residues in the positions 57-85 and, similarly to the Cys2-Cys2 motifs of the earlier considered γ-subunits of the archaeal initiation factors 2, this region comprises a separate subdomain, which contains two β-hairpins. However, the subdomain of SsoIF2γ is significantly different in the structure from the zinc fingers of other aIF2γ. It contains additionally three amino acid residues between the second and third cysteines and two aa after the fourth cysteine and is described by the formula 2x, C, 2x, C, 11x, C, 2x, C, 8x. The Cys2-Cys2 extension of the SsoIF2γ subdomain by five aa relative to the zinc fingers of the other aIF2γ causes significant change in its conformation in comparison with others.

Superposition of the SsoIF2γ and PabIF2γ subdomain structures is shown in Fig. 5. The insertion of three aa in the N-terminal β-hairpin of SsoIF2γ resulted in formation of the single-turn helix involving amino acid residues 64-68 and stabilized with two hydrogen bonds Lys63 O – Ala67 N and Pro65 O – Tyr68 N, whereas conformation of the remaining part of the hairpin was not essentially changed. Position of the Cα-atoms of cysteines is practically identical in both proteins. Insertion of two amino acid residues after the last cysteine in the C-terminal β-hairpin of the SsoIF2γ sequence changed conformation of the sequence at the 73-83 positions displacing both cysteines to the ends of the 74-78 single-turn helix. For the Cys77 of Cα this displacement was 3.91 Å relative to the corresponding Cys75 in PabIF2γ.

Convergence of cysteines of the N- and C-terminal hairpins in the Cys2-Cys2 subdomain of SsoIF2γ and change in the orientation of their Cα-Cβ bonds has led to formation of two S-S bridges, Cys59-Cys74 and Cys62-Cys77, stabilizing the subdomain structure. Comparison of the high-resolution SsoIF2γ structures has shown that the sulfur atoms are located in the apices of the irregular tetrahedral pyramid with the sides S59-S74 and S62-S77 equal to 2.05 ± 0.01 Å and the sides S59-S62, S59-S77, S62-S74, and S74-S77 equal to 4.80 ± 0.08, 3.92 ± 0.09, 5.42 ± 0.14, and 4.77 ± 0.07 Å, respectively. Obviously, in this case coordination of the sulfur atoms by the zinc atom is impossible, which is corroborated by the absence of zinc ion in all the SsoIF2γ structures.

Analysis of the SsoIF2γ crystal arrangements confirms high stability of the Cys2-Cys2 subdomain of this

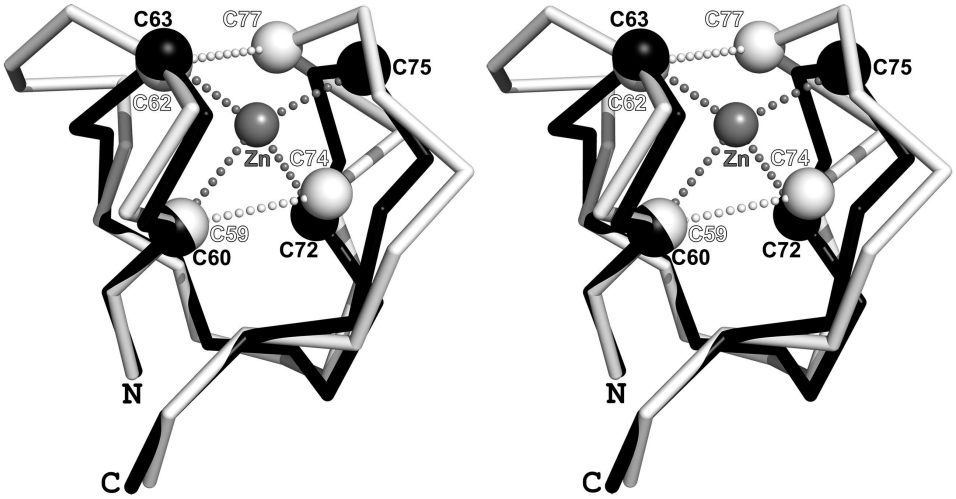


**Fig. 5.** Superposition of the structures of SsoIF2γ subdomains (shown in white, PDB-code: 4rd4) and of PabIF2γ (shown in black, PDB-code: 1kk3); the stereopairs. Amino acid residues at the positions 57-62, 67-70, and 82-85 of the 4rd4 structure and amino acid residues at the positions 58-63, 65-68, and 78-81 of the 1kk3 structure ($\sigma = 0.516$) are superimposed. The Cα-atoms of cysteines are shown by spheres of the corresponding colors, the zinc ion of PabIF2γ is shown as a gray sphere. Insertion of three amino acid residues into the N-terminal β-hairpin of SsoIF2γ and of two amino acid residues to the C-terminal β-hairpin resulted in formation of two single-turn helices 64-68 and 74-78, two S-S bonds, and a significant displacement of the hairpins relative to each other. For the Cys77 of Cα this displacement was 3.91 Å relative to the corresponding Cys75 of PabIF2γ.

protein, which contains two S-S bridges. The known by now SsoIF2γ structures are crystallized in nine spatial groups (table). Among the considered structures there are some corresponding to all three states of the protein (the GTP-bound, GDP-bound, and nucleotide-free), including those containing αγ-heterodimer and complex of the γ-subunit with the α1-helix belonging to the β-subunit. The highest density of the environment of the cysteine subdomain has been found in the crystal from the P1 spatial group. In this structure the subdomain contacts with two neighbor molecules: the hairpin β19-β20 of the domain III of one molecule and the interdomain constriction of the other molecule between domains II and III. The domain III of the neighboring molecule covers the cavity on the SsoIF2γ surface within the subdomain on which the binding site of the β-subunit is located. A similar contact with the domain III of the symmetric molecule has been found in the 4rjl crystal structure belonging to the cubic spatial group of symmetry I23, and in the 2pmd and 4m2l crystal structures belonging to the space groups P31 and P3121, respectively. In the rest of the SsoIF2γ- and SsoIF2αγ-heterodimer crystals the binding site of the β-subunit is also occupied by different parts of symmetric molecules, e.g., by the hairpin β12-β13, the N-terminal part of the switch 2, by the switch 1, or by the α-subunit domain 1. Only in crystals of the γ-subunit complex with the α1-helix belonging to the β-subunit (PDB-code: 2qn6) there are no intermolecular contacts in this region. Thus, it follows that the Cys2-Cys2 subdomain set boundaries to the "sticky" cavity on the γ-subunit surface, which is used for binding α1-helix of the β-subunit. Moreover, affinity of this helix for the γ-subunit is higher than the affinity of other regions of SsoIF2 involved in the crystal contacts.

Comparison of the SsoIF2γ structures belonging to different groups of symmetry has revealed that, despite the different environment, there are no significant changes in the conformation of the major chain of the Cys2-Cys2 subdomain with the change in the arrangement of molecules in the crystal (standard deviation is no more than 0.85 Å even for the pair of low-resolution structures). Displacement was the greatest for the Cα-atoms of the Cys77; the distance between these atoms in the low- or medium-resolution structures can reach 2.2 Å. However, it should be noted that this displacement virtually does not affect mutual arrangement of the sulfur atoms of all four cysteines, the distances between which remain practically unchanged. The subdomain region facing the molecule body (amino acid residues at positions 57-69) is its most conserved region.

The Cys2-Cys2 structure of the SsoIF2γ subdomain demonstrates that the presence of four closely located cysteines does not ultimately lead to the formation of a zinc finger. Unlike in the other aIF2γ, in the SsoIF2γ structure cysteines of two neighboring hairpins form two S-S bonds that provide high stability and prevent rearrangements in the locations of the sulfur atoms, which are necessary for docking of zinc ion. It may be concluded that part of the aIF2γ molecule, which exhibits a zinc finger shape in the PfuIF2γ, PabIF2γ, and MjaIF2γ structures, is not intended to perform the functions of this finger known from the literature, but is used only for creating binding site of the β-subunit. The SsoIF2γ subdomain, which does not require binding of zinc ion for stabilization, is more preferable for this purpose than the zinc finger used by the other archaea. Analysis of the corresponding regions of the amino acid sequences of the initiation factors 2 of yeast and human allows us to conclude that the specific for the SsoIF2γ insertion of five amino acid residues into the Cys2-Cys2 sequence of the subdomain is an evolutionary acquisition, which is used also by eukaryotes.

## DISCUSSION

It seems that the zinc finger of archaeal IF2β is necessary for additional protection of the nucleotide in the nucleotide-binding pocket and does not have a structural function. In the presence of coordinating zinc ion, the sulfur atoms of all the four cysteines retain their mutual positions unlike the finger conformation as a whole. Analysis of the structures of the C-terminal domains of β-subunits from various organisms allows us to suggest high lability of this fragment. Superposition of all Cα-atoms for the crystal structures of PfuIF2β and SsoIF2β gives σ = 1.6 Å, whereas for the structures obtained by the NMR method it is virtually impossible to perform superposition. In the absence of zinc ion, the finger is unable to retain the ordered structure, and its β-sheet is disrupted. The strand β3 initiates immediate contact with the N-terminal part of the switch 1 of aIF2γ [9] that leads to shifting of the zinc finger relative to the nucleotide-binding pocket of the γ-subunit and reduces the degree of protection of the nucleotide from collision with other molecules during Brownian motion, although does not prevent it completely. Apparently, absence of the zinc ions is just as critical for functioning of the zinc finger of IF2β as the replacement of one of the cysteines by another amino acid residue [18]. Protective role of the β-subunit zinc finger is confirmed also by the finding that mutations in this region increase the intrinsic rate of GTP hydrolysis in the IF2 from *S. cerevisiae* even in the absence of eIF5 [17]. Moreover, the cryo-EM structure of the complete initiator complex of the archaeal ribosome [28] also demonstrates that in the case when the tRNA anticodon is far from the ribosomal P-site, the β-subunit zinc finger is located across the nucleotide-binding pocket of the γ-subunit and moves aside with the codon-anticodon pairing eliminating additional protection of the nucleotide.

The Cys2-Cys2 motif is retained also in the sequences of the β-subunits of eukaryotes that speaks in

favor of the similarity of functions of these motifs in both domains of the life. It is assumed that in eukaryotes the β-subunit zinc finger together with the lysine repeats participate in the binding of mRNA [29]. Nevertheless, analysis of the archaeal ribosome structure in the state before the codon-anticodon binding and in the state of the codon–anticodon interaction [28] does not reveal any contacts between the β-subunit and mRNA.

In the γ-subunit the subdomain containing the Cys2-Cys2 motif sets a boundary at one side of a deep cavity that forms the β-subunit binding site, the other side of which is formed by the α4 helix. Such cavity is absent in the factors containing one subunit, such as EF-Tu [30]. Formation of the cavity in the heterotrimeric translation initiation factors 2 facilitates necessary orientation of the recognizing helix of the β-subunit that can be oriented only parallel to the β7 strand (Fig. 1). The use of a small but stable structure of the zinc finger as a boundary seems to be an evolutionary acquisition of some aIF2s accelerating formation of the heterotrimer. However, the structure of the zinc finger containing the Cys2-Cys2 motif is stable only in the presence of zinc ion [9, 27]. In archaea, which use the zinc finger as a wall of the β-subunit binding site, the βγ-heterodimer generation can be inhibited or very difficult in the case of zinc insufficiency in the cell leading to disruption of the aIF2 function. Apparently, this could be the reason for replacement of the subdomain zinc-mediated stabilization by stabilization due to formation of two S-S bonds in *S. solfataricus* during the evolution. Moreover, the N-terminal helix of the SsoIF2γ subdomain is perpendicular to the α5 helix and enhances its attachment to the body of the molecule. It is noteworthy that the conserved Tyr68 position (numbering according to SsoIF2γ nomenclature) is identical with respect to the helix α5 in all known aIF2γ structures, regardless of the subdomain conformation. This residue is a component of the hydrophobic core between the subdomain and the body of the molecule. Strengthening of the subdomain bond with α5 and reducing the distance between the subdomain and α4 increases the probability of recognition of the SsoIF2γ binding site by the β-subunit. It should be noted that the sequences of the γ-subunits of eukaryotes do not contain the Cys2-Cys2 motif, however, it is very likely that a similar region of their binding site with the β-subunit is also stabilized by S-S bonds. Thus, the yeast subunit sequence contains five cysteines with minimal distance of four amino acid residues between them, whereas the sequence of the human γ-subunit contains only three cysteines. Thus, it is very reasonable to assume that this subdomain performs only structural function. This conclusion is also confirmed by high stability of the zinc finger of the archaeal γ-subunit that fundamentally discriminates it from the zinc finger of the β-subunits, which apparently does not perform the structural function.

Our analysis has shown that conformations of the subdomains containing the Cys2-Cys2 motifs in γ-subunits of aIF2s from different organisms can be significantly different. Conformation of the zinc finger in three known aIF2γ in the presence of zinc ions is produced due to coordination of the zinc atom in the center of the regular tetrahedral pyramid by four sulfur atoms in its apices, whereas in the SsoIF2γ structure sulfur atoms form two S-S bonds and do not need zinc ion for stabilization of the subdomain. Thus, despite the similarity of the formulas describing amino acid sequences of the subdomains, the presence of the Cys2-Cys2 motif is not sufficient evidence of the presence of zinc finger in the structure.

**Funding.** The work was financially supported by the State Budget Project no. AAAA-A19-119122490038-8.

**Ethics declarations.** The authors declare no conflict of interests in financial or any other sphere. This article does not contain any studies with human participants or animals performed by any of the authors.

## REFERENCES

1. Zhang, W., Xu, C., Bian, C., Tempel, W., Crombet., L., et al. (2011) Crystal structure of the Cys2-His2-type zinc finger domain of human DPF2, *Biochem. Biophys. Res. Commun.*, **413**, 58-61, doi: 10.1016/j.bbrc.2011.08.043.
2. Cassandri, M., Smirnov, A., Novelli, F., Pitolli, C., Agostini, M., et al. (2017) Zinc-finger proteins in health and disease, *Cell Death Discov.*, **3**, 17071-17082, doi: 10.1038/cddiscovery.2017.71.
3. Marmorstein, R., Carey, M., Ptashne, M., and Harrisont, S. C. (1992) DNA recognition by GAL4: structure of a protein–DNA complex, *Nature*, **356**, 408-414, doi: 10.1038/356408a0.
4. Hall, T. M. (2005) Multiple modes of RNA recognition by zinc finger proteins, *Curr. Opin. Struct. Biol.*, **15**, 367-373, doi: 10.1016/j.sbi.2005.04.004.
5. Mackay, J. P., and Crossley, M. (1998) Zinc fingers are sticking together, *Trends Biochem. Sci.*, **23**, 1-4, doi: 10.1016/s0968-0004(97)01168-7.
6. Cho, S., and Hoffman, D. W. (2002) Structure of the β subunit of translation initiation factor 2 from the archaeon *Methanococcus jannaschii*: a representation of the eIF2β/eIF5 family of proteins, *Biochemistry*, **41**, 5730-5742, doi: 10.1021/bio11984n.
7. Schmitt, E., Blanquet, S., and Mechulam, Y. (2002) The large subunit of initiation factor aIF2 is a close structural homologue of elongation factors, *EMBO J.*, **21**, 1821-1832, doi: 10.1093/emboj/21.7.1821.
8. Yatime, L., Mechulam, Y., Blanquet, S., and Schmitt, E. (2007) Structure of an archaeal heterotrimeric initiation factor 2 reveals a nucleotide state between the GTP and the GDP states, *Proc. Natl. Acad. Sci. USA*, **104**, 18445-18450, doi: 10.1073/pnas.0706784104.
9. Stolboushkina, E., Nikonov, S., Nikulin, A., Blasi, U., Manstein, D. J., et al. (2008) Crystal structure of the intact archaeal translation initiation factor 2 demonstrates very high conformational flexibility in the alpha- and beta-subunits, *J. Mol. Biol.*, **382**, 680-691, doi: 10.1016/j.jmb.2008.07.039.

10. Kyrpides, N. C., and Woese, C. R. (1998) Archaeal translation initiation revisited: the initiation factor 2 and eukaryotic initiation factor 2B α-β-δ subunit families, *Proc. Natl. Acad. Sci. USA*, **95**, 3726-3730, doi: 10.1073/pnas.95.7.3726.
11. Roll-Mecak, A., Alone, P., Cao, C., Dever, T. E., and Burley, S. K. (2004) X-ray structure of translation initiation factor eIF2gamma: implications for tRNA and eIF2alpha binding, *J. Biol. Chem.*, **279**, 10634-10642, doi: 10.1074/jbc.M310418200.
12. Sokabe, M., Yao, M., Sakai, N., Toya, S., and Tanaka, I. (2006) Structure of archaeal translational initiation factor 2 betagamma-GDP reveals significant conformational change of the beta-subunit and switch 1 region, *Proc. Natl. Acad. Sci. USA*, **103**, 13016-13021, doi: 10.1073/pnas.0604165103.
13. Gutierrez, P., Osborne, M. J., Siddiqui, N., Trempe, J. F., Arrowsmith, C., and Gehring, K. (2004) Structure of the archaeal translation initiation factor aIF2β from *Methanobacterium thermoautotrophicum:* implications for translation initiation, *Protein Sci.*, **13**, 659-667, doi: 10.1110/ps.03506604.
14. Gamsjaeger, R., Liew, C. K., Loughlin, F. E., Crossley, M., and Mackay, J. P. (2007) Sticky fingers: zinc-fingers as protein-recognition motifs, *Trends Biochem. Sci.*, **32**, 63-70, doi: 10.1016/j.tibs.2006.12.007.
15. Erickso, F. L., Harding, L. D., Dorris, D. R., and Hanning, E. M. (1997) Functional analysis of homologs of translation initiation factor 2 γ in yeast, *Mol. Gen. Genet.*, **253**, 711-719, doi: 10.1007/s004380050375.
16. Donahue, T. F., Cigan, A. M., Pabich, E. K., and Valavicius, B. C. (1988) Mutations at a Zn(II) finger motif in the yeast eIF-2 β gene alter ribosomal start-site selection during the scanning process, *Cell*, **54**, 621-632, doi: 10.1016/s0092-8674(88)80006-0.
17. Huang, H. K., Yoon, H., Hanning, E. M., Donahue, T. F. (1997) GTP hydrolysis controls stringent selection of the AUG start codon during translation initiation in *Saccharomyces cerevisiae*, *Genes Dev.*, **11**, 2396-2413, doi: 10.1101/gad.11.18.2396.
18. Castilho-Valavicius, B., Thompson, G. M., and Donahue, T. F. (1992) Mutation analysis of the Cys-X2-Cys-X19-Cys-X2-Cys motif in the β subunit of eukaryotic translation initiation factor 2, *Gene Expr.*, **2**, 297-309.
19. Nikonov, O., Stolboushkina, E., Arkhipova, V., Kravchenko, O., Nikonov, S., and Garber, M. (2014) Conformational transitions in the γ subunit of the archaeal translation initiation factor 2, *Acta Crystallogr. D Biol. Crystallogr.*, **70**, 658-667, doi: 10.1107/S1399004713032240.
20. Yatime, L., Mechulam, Y., Blanquet, S., and Schmitt, E. (2006) Structural switch of the gamma subunit in an archaeal aIF2alpha gamma heterodimer, *Structure*, **14**, 119-128, doi: 10.1016/j.str.2005.09.020.
21. Jones, T. A., Zou, J. Y., Cowan, S. W., and Kjeldgaard, M. (1991) Improved methods for building protein models in electron density maps and the location of errors in these models, *Acta Crystallogr. A Found. Adv.*, **47**, 110-119, doi: 10.1107/s0108767390010224.
22. Nikonov, O., Stolboushkina, E., Nikulin, A., Hasenöhrl, D., Bläsi, U., et al. (2007) New insights into the interactions of the translation initiation factor 2 from archaea with guanine nucleotides and initiator tRNA, *J. Mol. Biol.*, **373**, 328-336, doi: 10.1016/j.jmb.2007.07.048.
23. Nikonov, O., Kravchenko, O., Arkhipova, V., Stolboushkina, E., Nikonov, S., and Garber, M. (2016) Water clusters in the nucleotide-binding pocket of the protein aIF2g from the archaeon *Sulfolobus solfataricus*: proton transmission, *Biochimie*, **121**, 197-203, doi: 10.1016/j.biochi.2015.11.029.
24. Dubiez, E., Aleksandrov, A., Lazennec-Schurdevin, C., Mechulam, Y., and Schmitt, E. (2015) Identification of a second GTP-bound magnesium ion in archaeal initiation factor 2, *Nucleic Acids Res.*, **43**, 2946-2957, doi: 10.1093/nar/gkv053.
25. Nikonov, O., Kravchenko, O., Nevskaya, N., Stolboushkina, E., Garber, M., and Nikonov, S. (2019) The third structural switch in the archaeal translation initiation factor 2 (aIF2) molecule and its possible role in the initiation of GTP hydrolysis and the removal of aIF2 from the ribosome, *Acta Cryst. D Biol. Crystallogr.*, **75**, 392-399, doi: 10.1107/S2059798319002304.
26. Schmitt, E., Panvert, M., Lazennec-Schurdevin, C., Coureux, P. D., Perez, J., et al. (2012) Structure of the ternary initiation complex aIF2-GDPNP-methionylated initiator tRNA, *Nat. Struct. Mol. Biol.*, **19**, 450-454, doi: 10.1038/nsmb.2259.
27. Gutierrez, P., Collet-Matillon, S., Arrwsmith, C., and Gehring, K. (2002) Zinc is required for structural stability of the C-terminus of archaeal translation initiation factor aIF2β, *FEBS Lett.*, **517**, 155-158, doi: 10.1016/s0014-5793(02)02610-8.
28. Coureux, P.-D., Lazennec-Schurdevin, C., Monestier, A., Larquet, E., Cladiere, L., et al. (2016) Cryo-EM study of start codon selection during archaeal translation initiation, *Nat. Commun.*, **7**, 13366-13375, doi: 10.1038/ncomms13366.
29. Laurino, J. P., Thompson, G. M., Pacheco, E., Castilho, B. A. (1999) The β subunit of eukaryotic translation initiation factor 2 binds mRNA through the lysine repeats and a region comprising the C2-C2 motif, *Mol. Cell Biol.*, **19**, 173-181, doi: 10.1128/mcb.19.1.173.
30. Berchtold, H., Reshetnikova, L., Riser, C. O., Schirmer, N. K., Sprinzl, M., and Hilgenfeld, R. (1993) Crystal structure of active elongation factor Tu reveals major domain rearrangements, *Nature*, **365**, 126-132, doi: 10.1038/365126a0.